MAPPING HOMOGENEOUS MARE BASALT UNITS IN THE ARISTARCHUS QUADRANGLE USING CLEMENTINE SPECTRAL PARAMETERS. F. ZHANG[1,2], Y. L. ZOU[1], Y. C. ZHENG[1], and X. H. FU[1,2], [1]National Astronomical Observatories, CAS, Beijing, A20 Datun Road, Chaoyang District, Beijing 100012, P.R. China, [2]Graduate University of CAS, Beijing, No.80 Zhongguancun East Road, Haidian District, Beijing, 100049. (fzhang@bao.ac.cn)

Introduction: The compositional distribution and the stratigraphy of the mare basalt units are important to our understanding of the composition of the lunar interior and its thermal evolution [1]. Previous work using Earth-based telescopes and remote sensing data revealed that basalt units flows around the Aristarchus Plateau exhibit a wide range of spectral characteristics [2], compositions [e.g., 3, 4], and ages [e.g., 5, 6, 7]. Some of the youngest geologic features on the moon has been identified in this region [8]. It is therefore necessary to accurately and detailly define and outline basalt units in order to place constrains on the stratigraphy and ages of these basalt flows around the Aristarchus Plateau, together with their mineralogical analysis, to understand how the mare volcanism evolved compositionally and spatially. For these purpose, we have mapped the mare basalts around the Aristarchus Plateau using the Clementine UV/VIS multi-spectral images, and construct their compositional variations. This abstract presents the result of basalt units around the Aristarchus Plateau, which locate in Oceanus Procellarum and is not far from Mare Imbrium. The temporal and spatial variations of the mare volcanism of this area are also discussed.

Data reduction: We used the Clementine UV/VIS data to produce a multispectral image of the Aristarchus Plateau area ~6.57 °N to 43.13 °N and ~29.54 °W to 67.5 °W. Individual basalt flows can be identified by spectral and chemical differences using Clementine UV/VIS data [9]. The data were processed at a resolution of 200m/pixel using the ENVI software program. In addition to the multispectral images, two false color images, FeO map and TiO_2 map (using the algorithms of [10], [11]) were generated. For the result to show, the recently released LRO USGS global mosic (LRO_WAC_Mosic_Global_303ppd.jp2; see figure 2; downloaded from: ftp://pdsimage2.wr.usgs.gov/) was used as the basemap for exhibiting our units defined.

Method: In this study, firstly, the boundaries of mare units were mapped using false color images and FeO and TiO_2 content maps. Previous used false color image (750/415 nm ratio assigned to red, 750/950 nm ratio to green, and 415/750 nm ratio to blue; e.g., [12]) and our new false color image (750 nm assigned to red, reflect overall albedo of material; 415/750 nm ratio to green, sensitive to Ti content; and 750/950 nm ratio to blue, sensitive to Fe content) were both used together. In the false color images, we distinguished mare units by the color difference, which correlates with the compositional difference between them. In our false color image, homogeneous units present different colors (e.g., Mare basalts are in green color and highland in red), texture (e.g., smooth, or in patches) or saturation levels.

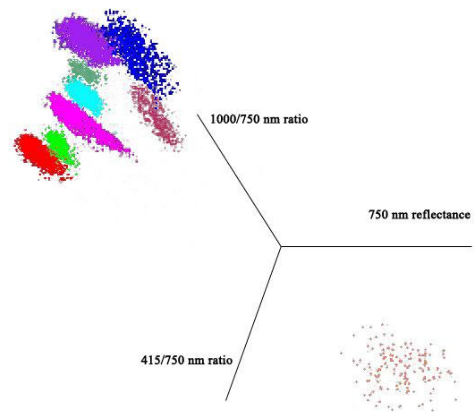

Figure 1: 3-dimensional scatter plot of some basalt units around the Aristarchus Plateau.

Clementine images provide these spectral measurements except for wavelengths near the absorption band around 2 μm. The albedo can be represented by the 750 nm reflectance, while the UV/VIS ratio is approximated by the 415/750 nm ratio, and the 1 μm absorption band is expressed by the 750/950 nm and 1000/750 nm ratios [13]. We derived these parameters by selecting pure pixels as regions of interest (ROIs) (e.g., natural clusters of data or end members that appeared in the viewer) from the Clementine images at 200 m/pixel spatial resolution for each unit. SubROIs can be distinguished on the basis of compositional and mineralogical differences [14]. Since the ejecta of a crater penetrating a surface mare unit contain materials of the underlying unit, the spectral parameters would be affected if these materials are included in the sampled area and their chemical composition is different from that of the surface unit. These materials can be distinguished from the surface basalts in the FeO and TiO_2 maps and the false color images. We carefully eliminated such craters and their ejecta from the sampled area to avoid contamination by these materials. We choose a ROI using a circle (coverage area is approximate 400 square kilometers) to obtain mean spectral parameters and FeO, TiO_2 content for each unit. Then, a 3 or 4-dimensional scatter plot (see Figure 1) is obtained using the 750 nm reflectance, 415/750 nm ratio, 750/950 nm ratio or (and) 1000/750 nm ratio as three (four) axes in spatial distribution. At last, the SAM (spectral angel mapper) supervised classification method is applied to units subgroups division.

Results: The distribution of mare basalts derived in this study is not only consistent with the previous studies [e.g., 2, 12], but also includes several new geological groups and subgroups. Totally, about 19 distinct basalt units (Figure 2 and Table 1) were defined in study region. The high-Ti basalts (2, 4, 5, 6, 7, 8; >9% TiO_2) are exposed in west part of the Aristarchus Plateau. They are youngest in these maria as indicated by the previous studies [15]. Application of these dataset in our study result in estimates of approximately 6-10 wt% TiO_2 for the most of hDSA basalts, and approximately 8-14 wt% TiO_2 for HDSA basalts. LBSP, LBG- types are to the north, which are close to the highland surrounding the Montes Jura. Another basalt type mISP located outside of the hDSA and HDSA type basalt units, occupying the western part of the study region. One special basalt unit 7, in which cone and dome spread all over, were classified as Cone and dome material by *Pieters* [1978]. FeO and TiO_2 contents of the unit are very high (FeO, 22.80 wt%; TiO_2, 12.47 wt%). In geologic map of the near side of the moon [16], the unit 7 was classified as Emp (Eratosthenian System) unit.

Table 1. Chemical composition of mare units in the study area derived from Clementine UVVIS data.

unit	FeO (wt%)	TiO_2 (wt%)	Pieters (1978)
1	19.89	7.63	hDSA
2	21.11	9.13	HDSA
3	19.62	7.13	hDSA
4	21.60	11.21	HDSA
5	21.96	10.30	hDSA
6	22.95	13.11	HDSA
7	22.80	12.47	Cone and dome material
8	22.68	11.27	hDSA
9	21.57	8.62	hDSA
10	21.69	7.43	hDSA, Undivided
11	17.88	2.17	LBSP
12	20.88	8.05	HDSA
13	20.34	6.22	hDSA
14	19.64	3.68	LBSP
15	21.05	7.00	hDSA
16	19.19	2.97	LBSP
17	17.69	1.88	Dark mantling material
18	18.74	4.41	LBSP, LBG-
19	17.36	4.23	LBG-

Our study also shows that basalt in Mare Imbrium have relatively lower Ti contents than the units distributed in Oceanus Procellarum. The high FeO contents range of these units suggest that the strong mafic band exhibited by the western high-Ti basalts indicates that they have a substantially higher iron content [17].

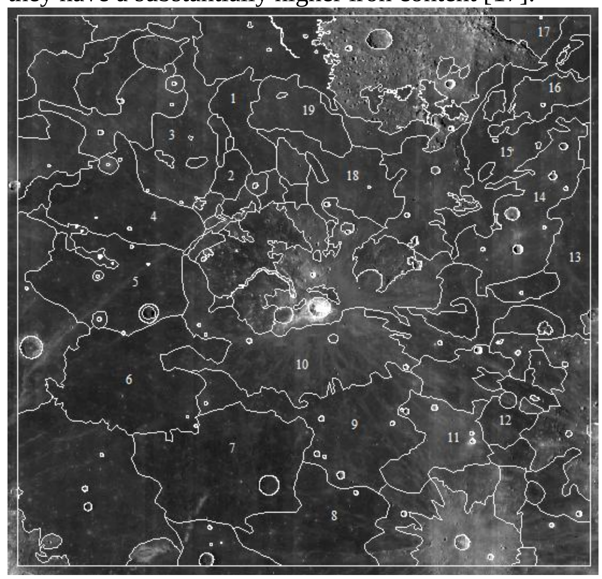

Figure 2: Homogeneous basalt units defined and outlined in the Aristarchus Quadrangle in our work.

Future work: This initial study of lunar basalt types focuses on one region (the Aristarchus Plateau quandrangle) of western nearside mare units. The approach will later be expanded to include other Mare Imbrium and Oceanus Procellarum basalt types.

References: [1] Kodama S. and Y. Yamaguchi (2005) LPS XXXVI, abstract #1641. [2] Pieters, C.M. (1978) PLPSC 9th, 2825-2849. [3] Lucey, P. G. et al. (2000) JGR, 105, 20297-20305. [4] Elphic, R. et al. (2002) JGR, 107, 5024-5031. [5] Boyce, J. M. (1976) PLSC 7th, 2717-2728. [6] Wilhelms, 1987, U.S. Geol. Surv. Prof. Pap. 1348. [7] Hiesinger, H. et al. (2003) JGR, 108. [8] Hiesinger, H. et al. (2008) LPS XXXIX, abstract #1269. [9] Nozette et al. (1994) Science 266, 1835-1839. [10] Lucey, P. G. et al. (1998) JGR, 103, 3679-3699. [11] Gillis, J. J. et al. (2003) JGR, 108, 3.1-3.18. [12] Hiesinger, H. et al. (2000) JGR, 105, 29239-29275. [13] Staid and Pieters, (2001) JGR, 106, 27887-27900. [14] Flor, E. L. (2003) LPS XXXIV, abstract #2086. [15] Pieters, C. M. (1980) JGR, 85, 3913-3938. [16] Wilhelms and McCauley (1971), I-703, USGS. [17] Taylor, G. J. et al. (1991) Lunar rocks, in Lunar sourcebook: A User's Guide to the moon, Cambridge Univ. Press, New York.